

# VeriDrive: Verifiable Counterfactual Supervision for Cost-Efficient Vision-Language Planning

Zikai Zhang

zikai.zhang@durham.ac.uk

Hubert P. H. Shum

hubert.shum@durham.ac.uk

Toby P. Breckon

toby.breckon@durham.ac.uk

Department of Computer Science

Durham University

Stockton Road, Durham, DH1 3LE, UK

---

## Abstract

Vision-language driving models increasingly use reasoning supervision to bridge perception, prediction, and planning, but existing driving rationales are often free-form and expensive to generate with frontier models. We present VeriDrive, a framework for constructing planning-oriented, verifiable counterfactual supervision. VeriDrive converts driving reasoning into a structured Perception–Evaluation–Revision chain that grounds key objects in future motion, evaluates alternative ego trajectories with rule-checkable evidence, revises risky intent toward expert behavior, and produces final planning targets. To scale data construction, VeriDrive combines local generation with validator-guided selective correction, escalating only invalid or difficult samples. We build the VeriDrive dataset on nuScenes and train under the Omni-Q protocol. Controlled open-loop experiments show that VeriDrive improves L2, Collision, and Intersection over OmniDrive while reducing logged token usage, generation time, and estimated paid GPT API cost under the stated pricing basis. These results show that auditable intermediate fields and structured revision targets can improve vision-language planning supervision under realistic annotation budgets. *Code, prompts, and validator scripts will be released in a future public repository.*

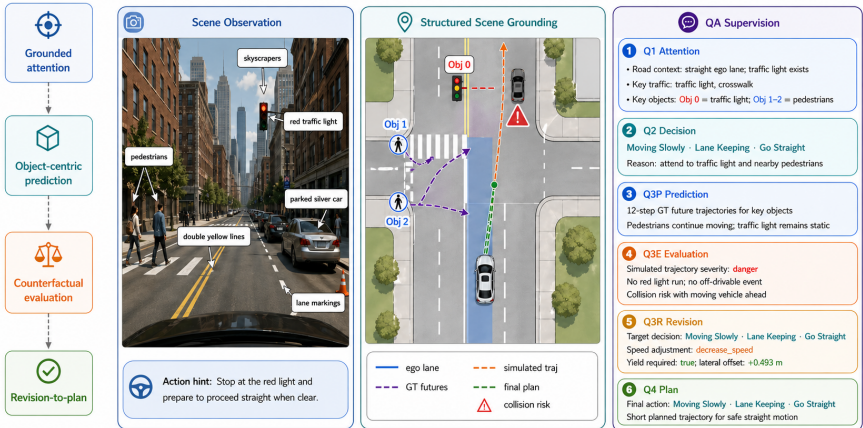


Figure 1: Structured QA example from VeriDrive, linking scene evidence to a verifiable reasoning chain. **(left)** the multi-view scene observation with highlighted driving cues; **(middle)** the bird’s-eye-view scene grounding with key objects, their future motion, and the simulated and final-plan ego trajectories; **(right)** the serialized Q1–Q4 Perception–Evaluation–Revision QA supervision chain.

## 1 Introduction

Recent advances in vision-language models (VLMs) have motivated a growing line of research on autonomous driving, where language-conditioned reasoning is used to bridge perception, prediction, and planning in a more interpretable manner. Representative works such as those in [20] cast autonomous driving as a structured visual question answering problem and show that explicit reasoning over perception, prediction, and planning can improve decision making in complex scenes. More recently, work such as [24] further demonstrates that *counterfactual* supervision—evaluating how alternative ego trajectories would change future risk—provides a promising route to align VLMs with planning-oriented driving behavior. These results suggest that the quality of supervision, rather than model scale alone, is becoming a central factor for vision-language planning in autonomous driving.

At the same time, recent driving-VLM research has increasingly moved from direct answer generation toward structured reasoning pipelines that explicitly connect perception, prediction, and planning [20, 27]. However, current planning-oriented driving datasets still face two important challenges. First, many reasoning traces are expressed as free-form natural language, which makes the intermediate chain of thought difficult to verify, hard to audit, and weakly grounded in explicit scene evidence. In practice, this often causes a mismatch between the generated explanation and the actual planning factors that determine safety-oriented open-loop planning outcomes. Second, high-quality data construction increasingly relies on expensive frontier LLM/VLM models [17, 20, 24], making large-scale supervision costly and limiting reproducibility. While prior work in [24] shows that counterfactual reasoning can substantially improve autonomous-driving VLM, the corresponding data construction pipeline still depends on powerful generators and does not explicitly enforce verifiable intermediate supervision throughout the reasoning process.

These observations motivate a different view of planning-oriented supervision: it should be both *verifiable* and *budget-aware*. Instead of treating chain-of-thought as a free-form

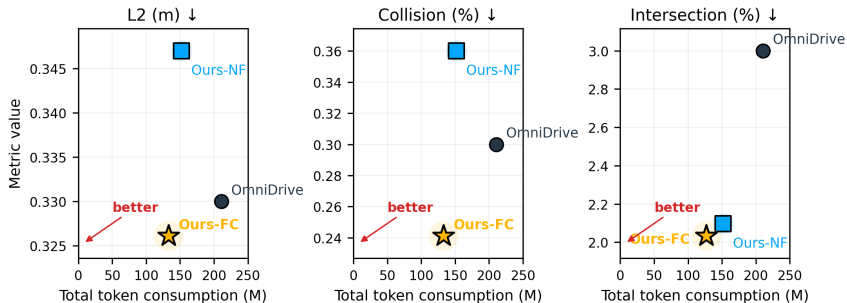


Figure 2: Efficiency–performance trade-off on nuScenes open-loop planning. Panels plot average planning metrics against logged generation-token consumption; lower-left is better. OmniDrive is the counterfactual QA baseline, while Ours (no filter) and Ours (filter) denote VeriDrive without and with validator-routed filtering/correction. Plot aliases Ours-NF and Ours-FC correspond to Ours (no filter) and Ours (filter), respectively.

textual artifact, we argue that the intermediate reasoning process should be constrained by structured evidence that can be checked by annotations or deterministic rules. Meanwhile, if high-quality generation is only necessary for invalid or difficult cases, then expensive frontier LLM/VLM models need not be used uniformly across all samples. The central question of this work is therefore how to construct a supervision framework that preserves the interpretability of driving reasoning, strengthens its grounding in planning-critical evidence, and remains scalable under realistic query budgets.

To answer this question, we propose a **verifiable counterfactual supervision framework** that reformulates planning-oriented reasoning as a structured Perception–Evaluation–Revision process. Our key idea is to explicitly supervise three stages of counterfactual reasoning: (1) grounding future interaction evidence on the key traffic participants selected from the scene, (2) evaluating simulated ego trajectories with rule-grounded risk analysis, and (3) revising invalid or risky decisions toward expert behavior through structured intent-level correction. Based on this framework, we construct the **VeriDrive dataset**, a planning-oriented dataset with auditable intermediate supervision, including structured attention grounding, object-centric future motion evidence, rule-based counterfactual evaluation, and expert-guided revision. To make dataset construction scalable, we further develop a budget-aware generation pipeline that combines a low-cost local generator with validation-driven selective correction, so that expensive high-quality generation is reserved only for samples that are invalid or difficult. Figure 2 previews this trade-off: the validator-routed VeriDrive variant improves the reported open-loop metrics while using fewer logged generation tokens than the OmniDrive-style baseline under the same accounting. Figure 1 illustrates the resulting supervision format, showing how scene evidence, future grounding, counterfactual risk evaluation, revision, and final planning are serialized into one auditable Question-Answer chain.

We evaluate VeriDrive on nuScenes open-loop planning using the Omni-Q setting [24]. The results show that the proposed dataset and supervision protocol improve planning performance, especially on Collision and Intersection, while reducing logged token/time overhead and estimated paid GPT API cost. Following the closest driving-VLM supervision protocols, our empirical claims are limited to this open-loop protocol and its safety-proxy metrics rather than closed-loop deployment safety.

The key novel contributions of our work are three-fold:

- We propose **VeriDrive**, a framework that makes planning-oriented driving CoT verifiable and corrective through future-risk grounding, rule-violation checking, and unsafe-plan revision before final planning.
- We construct the **VeriDrive dataset** on top of nuScenes and introduce a **budget-aware generation pipeline** that combines compact scene conditioning, low-cost local generation, dual validation, and selective high-quality correction.
- We demonstrate that the resulting dataset and supervision improve nuScenes open-loop planning. In a controlled comparison against OmniDrive [24] under the same setting, VeriDrive yields consistent gains on L2, Collision, and Intersection while simultaneously reducing logged token usage, wall-clock generation time, and estimated paid GPT API cost.

## 2 Related Work

**End-to-end autonomous driving.** Planning-oriented end-to-end driving methods optimize ego behavior directly from scene observations. UniAD [8] jointly models perception, prediction, and planning, while VAD [10] improves planning with vectorized agent and map representations. BEV-Planner [13] and recent analyses of nuScenes open-loop evaluation [23] further show that strong open-loop trajectory metrics do not necessarily imply complete scene understanding or closed-loop behavior. These works motivate richer supervision beyond pure trajectory imitation, but their supervision remains primarily geometric and provides limited explicit evidence about why a plan violates constraints or how it should be revised.

**Driving vision-language models.** Recent driving VLM use language to expose intermediate decision factors. DriveLM [21] formulates driving as graph visual question answering over perception, prediction, behavior, and planning. DriveVLM [22] and AutoDrive-P<sup>3</sup> [27] further connect language reasoning with planning-oriented supervision and perception–prediction–planning thought. However, many intermediate rationales remain free-form natural language, making them difficult to audit, weakly tied to explicit scene evidence, and hard to verify programmatically.

**Driving datasets and supervision generation.** Language-centric driving datasets have progressed from explanation and command-following resources such as Talk2Car [6], BDD-X [11], HDD [19], DRAMA [15], and Rank2Tell [20] to larger QA and reasoning datasets such as nuScenes-QA [18], NuPrompt [25], LingoQA [16], Reason2Drive [17], DriveLM [21], and OmniDrive [24]. These datasets broaden language grounding in driving from scene description and object-centric prompts to graph QA, chain-based reasoning, and counterfactual planning supervision. Recent works also expose the need for scalable supervision generation and evaluation: LingoQA [16] studies answer truthfulness with a learned judge, while OmniDrive [24] constructs counterfactual QA from simulated and actual trajectories. However, existing driving-language datasets usually emphasize QA scale, reasoning format, or downstream accuracy, while providing limited analysis of whether the generated intermediate fields are programmatically checkable and how token usage, generation time, and cost vary under different generation policies. VeriDrive targets this gap by coupling structured validators with selective correction for planning-oriented counterfactual supervision.

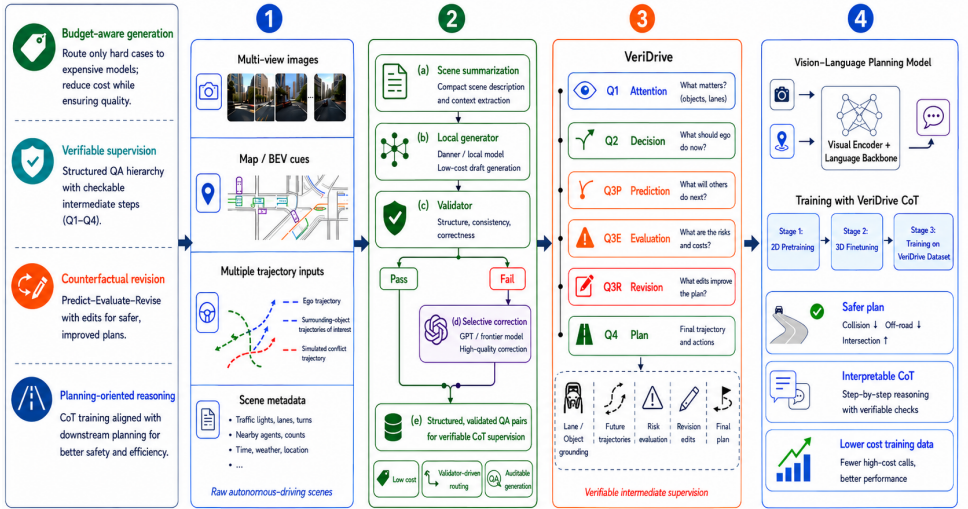


Figure 3: Overview of VeriDrive. Given multi-view images, map/BEV cues, candidate ego trajectories, and scene metadata, VeriDrive constructs compact scene evidence, applies local generation, validation, and selective correction, then serializes the Q1–Q4 Perception–Evaluation–Revision chain for Stage-3 Omni-Q fine-tuning.

## 3 Methodology

VeriDrive consists of three coupled components: verifiable counterfactual supervision, budget-aware query routing and correction, and Stage-3 fine-tuning under the OmniDrive [24] baseline setting. The first constrains intermediate reasoning with rule-checkable evidence, the second allocates expensive queries only when validation indicates a need, and the third serializes the resulting evidence and revision targets for planning supervision.

### 3.1 Overview

Figure 3 presents the main contribution overview. Given a driving scene represented as  $\mathbf{s} = \{\mathcal{X}_{\text{scene}}, \mathcal{O}, \mathcal{M}, \tau^{\text{sim}}, \tau^*\}$ , our goal is to construct a structured supervision tuple,  $\mathcal{Q} = \{Q_1, Q_2, Q_{3P}, Q_{3E}, Q_{3R}, Q_4\}$ , which remains planning-informative while keeping intermediate evidence verifiable. Here  $Q_1$  denotes compact planning-oriented scene evidence,  $Q_2$  denotes the ego meta action,  $Q_{3P}$  denotes object-centric future motion grounding,  $Q_{3E}$  denotes rule-grounded counterfactual evaluation,  $Q_{3R}$  denotes the revision target, and  $Q_4$  denotes the final expert planning target. For brevity, we refer to  $\{Q_{3P}, Q_{3E}, Q_{3R}\}$  collectively as the  $Q_3$  block when discussing the supervision structure. The precise training/inference serialization protocol is summarized in Sec. 3.4 and described in more detail in the supplementary.

Instead of relying on free-form chain-of-thought, VeriDrive organizes supervision as an explicit Perception–Evaluation–Revision pipeline in which planning-critical variables are either directly derived from annotations or computed by deterministic rules. Language is mainly used to package verified evidence into canonical QA supervision rather than to hallucinate unconstrained reasoning traces.

## 3.2 Verifiable Counterfactual Supervision

**Relation to OmniDrive.** We use the Omni-Q training protocol and follow the OmniDrive high-level counterfactual trajectory construction principle to enable a controlled comparison. The contribution of VeriDrive is not a new planner or a replacement for the OmniDrive simulated trajectory generation. Instead, VeriDrive changes the supervision interface:  $Q_{3P}$  grounds key objects in future motion,  $Q_{3E}$  converts counterfactual outcomes into rule-checkable risk fields, and  $Q_{3R}$  supervises expert-aligned intent revision. This separation enables programmatic diagnostics and validator-routed correction, which are evaluated in Secs. 4.3 and 4.6.

To create auditable planning-oriented reasoning, we reformulate the supervision as a structured chain:

$$Q_1 \rightarrow Q_2 \rightarrow Q_{3P} \rightarrow Q_{3E} \rightarrow Q_{3R} \rightarrow Q_4,$$

where each stage is grounded either in annotations or in deterministic rule-based computation. This design follows the general perception–prediction–planning reasoning principle in recent driving VLM [21, 27], while explicitly emphasizing verifiability and revision supervision. In particular, our simulated trajectory generation and conflict checking adopt the same counterfactual construction principle as OmniDrive, which uses rule-based checklists to evaluate the open-loop risk consequences of candidate trajectories [24].

### 3.2.1 Planning-oriented evidence construction

We first construct a compact planning-oriented evidence space from the raw scene. Rather than exposing all scene objects to the reasoning pipeline, we represent each sample by:

$$\mathcal{C}_n = \left\{ \mathcal{C}_n^{\text{road}}, \mathcal{C}_n^{\text{traffic}}, \mathcal{O}_n^{\text{key}} \right\}, \quad (1)$$

where  $\mathcal{C}_n^{\text{road}}$  denotes the ego-lane context,  $\mathcal{C}_n^{\text{traffic}}$  contains planning-relevant traffic-control elements, and  $\mathcal{O}_n^{\text{key}}$  is the set of selected key objects. This compact representation simultaneously serves two purposes: it defines the attention-grounded evidence space for counterfactual reasoning, and it reduces prompt redundancy during data generation.

We score candidate objects by lane relevance, interaction proximity, vulnerable-road-user priority, and traffic-control coupling, and retain the top- $K$  objects as  $\mathcal{O}_n^{\text{key}}$ . This compact evidence space bounds later reasoning to traceable scene elements and reduces prompt redundancy. Detailed scoring weights and implementation are provided in the supplementary material. In addition, the high-level ego behavior is represented as a meta action  $a_n^{\text{ego}} \in \mathcal{A}$ , where  $\mathcal{A}$  denotes commands such as lane keeping, going straight, yielding, or slowing down.

### 3.2.2 Object-centric future motion grounding

To make the selected key objects usable for counterfactual reasoning, we associate each of them with a short-horizon future trajectory:

$$\mathcal{P}_n = \left\{ (i, \mathbf{y}_i^*) : o_i \in \mathcal{O}_n^{\text{key}} \right\}, \quad (2)$$

where  $\mathbf{y}_i^*$  denotes the future trajectory of object  $i$  over the prediction horizon. This step transforms object-centric attention into future interaction evidence: the model is not only

told which objects matter, but also how they are expected to evolve. As a result, later counterfactual evaluation becomes explicitly tied to the motion of attended agents rather than to static scene cues alone.

### 3.2.3 Rule-grounded counterfactual evaluation

Following OmniDrive [24], we construct candidate simulated ego trajectories  $\tau_n^{\text{sim},m}$  and evaluate them with rule-based checklists for counterfactual supervision. Given a simulated trajectory, the evaluator receives as input the planning-oriented evidence space and the future trajectories of the selected key objects, and returns structured risk signals such as collision, out-of-drivable-area status, traffic-light violation, severity, and triggering evidence:

$$\mathcal{Z}_n^{(m)} = g\left(\tau_n^{\text{sim},m}, \mathcal{C}_n^{\text{traffic}} \cup \mathcal{P}_n, \mathcal{M}_n\right). \quad (3)$$

The key property of this stage is that counterfactual explanations must be grounded in already selected evidence. If a collision occurs, the explanation is explicitly tied to the future trajectory of a key object in  $\mathcal{P}_n$  rather than to an unconstrained textual rationale. Similarly, map-based violations such as red-light running or leaving the drivable region are determined from map and traffic-control constraints. This converts counterfactual reasoning from free-form explanation into evidence-based risk attribution.

### 3.2.4 Expert-aligned revision and final planning target

After the simulated behavior has been evaluated, we do not directly replace it with the expert trajectory. Instead, we first revise the *intent-level decision*. Let  $a_n^{\text{sim},m}$  denote the meta action associated with the simulated trajectory, and let  $a_n^*$  be the expert meta action extracted from the expert trajectory. We then supervise the revision target as:

$$\mathcal{R}_n^{(m)} = \left(a_n^*, \mathcal{U}_n^{(m)}\right), \quad (4)$$

where  $\mathcal{U}_n^{(m)}$  is the set of evidence references justifying the revision, restricted to the same evidence space used in evaluation.

This means that the revision stage changes only the high-level intent—for example, whether the vehicle should yield, decelerate, or continue lane-following—while the final geometric trajectory is deferred to the last stage. The final planning target is simply the expert trajectory  $Q_{4,n} = \tau_n^*$ . Compared with direct trajectory imitation, this decomposition provides a more controllable supervision signal: the model must first infer why a simulated decision is wrong and which intent-level correction is required before generating the final expert-aligned plan.

## 3.3 Budget-Aware Data Generation

Although frontier LLM/VLM models can produce stronger structured annotations, applying them uniformly is prohibitively expensive and often unnecessary for simple scenes. We therefore combine a low-cost local branch with validation-driven selective correction and reuse the compact evidence space from Sec. 3.2.1 to reduce prompt redundancy. The overall workflow is already summarized in Figure 3, so we describe the routing and validation details directly below without introducing a separate pipeline figure.

### 3.3.1 Cost-aware routing and dual validation

For each scene  $\mathbf{s}_n$ , we consider two candidate generation branches: a low-cost local branch and a high-quality correction branch:

$$\hat{Q}_n = \begin{cases} G_{\text{loc}}(\mathbf{s}_n), & a_n = 0, \\ G_{\text{hq}}(\mathbf{s}_n), & a_n = 1, \end{cases} \quad (5)$$

where  $a_n \in \{0, 1\}$  is the routing variable.

The routing decision is driven by a dual validator composed of a hard-constraint branch and a complexity branch. The hard-constraint branch checks whether the local output satisfies mandatory format and attention requirements, yielding a hard failure flag:

$$z_n = \mathbb{I}(m_{n,\text{format}} \cdot m_{n,\text{attn}} = 0), \quad (6)$$

where  $m_{n,\text{format}}, m_{n,\text{attn}} \in \{0, 1\}$  denote format validity and attention completeness, respectively. In parallel, we compute a continuous complexity score  $\rho_n \in [0, 1]$ , summarizing scene density, interaction intensity, traffic-control complexity, and attention incompleteness. A sample is escalated whenever the local output is structurally invalid or sufficiently complex:

$$a_n = \mathbb{I}(z_n = 1 \vee \rho_n \geq \tau_\rho). \quad (7)$$

This design ensures that invalid samples are always repaired, while expensive correction is reserved for hard-but-valid cases only when their estimated complexity is high.

### 3.3.2 Budget-constrained selective correction

The correction ratio is controlled by a user-defined budget. We rank locally generated samples using validator-derived utility and escalate the most valuable samples until the budget is exhausted. This enables the same pipeline to operate under different token, latency, or monetary constraints while still allowing high-quality supervision for invalid or difficult cases.

## 3.4 Training Strategy

We follow the original OmniDrive training pipeline to keep the backbone and optimization recipe unchanged, such that the performance gain can be primarily attributed to our supervision design. Specifically, we initialize from the OmniDrive baseline [24], and follow the same Stage-1 (2D pretraining) and Stage-2 (3D finetuning) settings as the original framework. Finally, we further fine-tune the model on our structured driving supervision data.

During Stage-3 training, we use verified intermediate supervision as teacher-forced context and targets. Specifically, the structured sequence is organized as:

$$Q_1 \rightarrow Q_2 \rightarrow Q_{3P} \rightarrow Q_{3E} \rightarrow Q_{3R} \rightarrow Q_4.$$

The verified intermediate fields are used during training to expose the model to object-grounded future motion evidence, rule-grounded counterfactual evaluation, and expert-aligned revision supervision. This design improves supervision quality but does not change the test-time information available to the model.

At inference time, we follow a no-oracle autoregressive rollout. The model is given only the normal scene observation inputs used by the Omni-Q setting, together with current

ego/map context when available in the baseline protocol. It then sequentially generates:  $\hat{Q}_1 \rightarrow \hat{Q}_2 \rightarrow \hat{Q}_{3P} \rightarrow \hat{Q}_{3E} \rightarrow \hat{Q}_{3R} \rightarrow \hat{Q}_4$ .

Ground-truth future object trajectories, rule-evaluation labels, expert meta-actions, and revision targets are not provided during evaluation. Therefore,  $Q_{3P}$  and  $Q_{3E}$  serve as training-time supervision for learning structured reasoning, not as oracle test-time inputs. All planning results reported in Sec. 4.4 are obtained under this no-oracle autoregressive inference protocol unless explicitly marked as oracle or teacher-forced analysis. Additional engineering details are deferred to the supplementary material.

## 4 Experiments

We evaluate whether the proposed supervision improves planning quality under the same model setting, and whether the generation pipeline lowers the cost of producing that supervision, focusing on planning metrics, component ablations, and generation efficiency.







### 4.1 Implementation Details

We adopt the Omni-Q architecture following OmniDrive [24], with EVA-02-L [6] as the visual encoder and a LLaVA v1.5-based language backbone [24]. Stage-1 (2D pretraining) and Stage-2 (3D finetuning) follow the original OmniDrive recipe, and Stage-3 further fine-tunes on the VeriDrive dataset. Unless stated otherwise, rule-based filtering constrains  $K \leq 5$ . Evaluation follows the no-oracle autoregressive rollout in Sec. 3.4, with no ground-truth  $Q_2$ ,  $Q_{3P}$ ,  $Q_{3E}$ , or  $Q_{3R}$  injected at test time. For data generation, the local branch uses Qwen3-VL-32B-Instruct [1], while the high-quality correction branch uses GPT-5.5; the exact model and pricing basis are reported in the supplementary material and Table 6. Unless otherwise stated, the validator complexity threshold is 0.65, and the default routing setting escalates approximately 30% of samples to the high-quality correction branch. The complexity score combines scene density, interaction intensity, traffic-control complexity, and attention incompleteness. Stage-3 fine-tuning uses 2 epochs, learning rate  $2 \times 10^{-5}$ , batch size 4, and the same backbone and optimization recipe as OmniDrive unless otherwise specified. Representative serialization details, validator thresholds, routing settings, generator/judge settings, and additional hyperparameters are provided in the supplementary material. Full prompt templates and scripts will be released with the future public code repository.

### 4.2 Dataset & Metrics

**NuScenes Dataset.** We conduct our study on top of the nuScenes benchmark [2], which contains 1,000 driving scenes of approximately 20 seconds each with synchronized multi-modal sensor recordings, including 6 cameras, 5 radars, and 1 LiDAR, together with 3D box annotations for 23 semantic classes and 8 attributes. Originally introduced for 3D detection and tracking, nuScenes has since become a standard testbed for downstream autonomous-driving tasks, including open-loop planning. Built upon nuScenes, OmniDrive [24] extends the benchmark to the vision-language setting by introducing a holistic driving dataset with counterfactual reasoning. It constructs QA supervision from simulated and actual trajectories, and explicitly aligns language-based reasoning with 3D driving tasks such as scene understanding, decision making, and planning.

Table 1: Comparison of representative language-centric driving datasets:  $\checkmark$  = *explicit support*,  $\triangle$  = *partial support*,  $-$  = *no support*; *MV* = *multi-view input*, *CF* = *counterfactual reasoning*, *3D* = *explicit 3D or multi-modal geometry*; *Plan* = *planning-oriented supervision*; *Veri.* = *checkable structured fields rather than human-verified explanation faithfulness*; *Edit Sup.* = *denotes revision or correction targets*.

Dataset	Input	Scale	Text supervision	3D	Plan.	CF	Reasoning	Veri.	Edit Sup.
BDD-X 	Front-view video	6.9k clips / 26k texts	Description + explanation	-	-	-	Free-form	-	-
BDD-OIA 	Driving scenes	22.9k scenarios / 35k ann.	Action + explanation	-	$\triangle$	-	Explanation labels	-	-
NuScenes-QA 	MV + LiDAR	34k scenes / 460k QA	Template QA	$\checkmark$	-	-	Template	$\triangle$	-
DriveLM 	MV + 3D	30k scenarios / 443k QA	Graph QA for perception, prediction, and planning	$\checkmark$	$\checkmark$	-	Graph	-	-
LingoQA 	Front-view video	28k videos / 419.9k QA	Free-form QA + justification	-	$\triangle$	$\triangle$	Free-form	-	-
OmniDrive 	MV + 3D	34.1k scenes / 480.4k QA	QA + counterfactual reasoning	$\checkmark$	$\checkmark$	-	Counterfactual	$\triangle$	-
VeriDrive dataset (ours)	MV + 3D	33.1k samples / 198.8k QA	Verifiable QA + edit traces	$\checkmark$	$\checkmark$	$\checkmark$	Step-based	$\checkmark$	$\checkmark$

**VeriDrive dataset.** We apply the VeriDrive framework to NuScenes and construct the VeriDrive dataset, a planning-oriented dataset with verifiable counterfactual supervision. The VeriDrive dataset contains 27,271 training samples and 5,868 validation samples after filtering out all samples without valid expert trajectories. Each sample is organized as a structured supervision tuple covering perception, decision, counterfactual evaluation, revision, and final planning targets. In particular, the perception-related QA annotations are derived automatically from nuScenes and OpenLane-V2 [23] ground truth, the ego future trajectory is represented by 6 steps, and each selected surrounding object is associated with a 12-step future trajectory for interaction grounding. Unlike nuScenes, which mainly provides raw sensory and geometric annotations, and OmniDrive, which relies on counterfactual QA generation, the VeriDrive dataset explicitly introduces auditable intermediate supervision and expert-guided revision signals throughout the reasoning chain. The full annotation process is fully scripted and scalable (hence repeatable), and produces structured reasoning traces with explicit explanations that better align with object- and rule-grounded planning supervision. Table 1 positions VeriDrive among representative language-centric driving datasets.

Compared with prior QA or explanation datasets, VeriDrive emphasizes planning-oriented supervision with explicit counterfactual evaluation, programmatic verifiability, and expert-aligned edit traces. The comparison is intended to clarify the dataset contribution and supervision design rather than to imply that scale alone determines annotation quality.

**Evaluation metrics.** Following OmniDrive [24] and BEV-Planner [13], we evaluate planning performance in the nuScenes open-loop setting using three metrics: L2 displacement error, Collision Rate, and Intersection Rate. L2 measures the geometric deviation between the predicted ego trajectory and the expert trajectory, reflecting trajectory fitting accuracy. Collision Rate measures whether the predicted trajectory collides with surrounding objects, and therefore provides an open-loop collision proxy with respect to dynamic traffic participants. Intersection Rate measures whether the predicted trajectory violates the drivable region or intersects the road boundary, capturing map compliance and road-structure awareness. In our analysis, we place particular emphasis on Collision Rate and Intersection Rate, since these two metrics more directly reflect safety-oriented open-loop planning behavior than geometric error alone.

### 4.3 Verification Diagnostics

Table 2 summarizes programmatic checks for dataset-level validity and no-oracle rollout validity. Dataset-generation diagnostics are computed on the final retained VeriDrive samples after selective correction, whereas no-oracle diagnostics are computed from validation-set

rollout outputs. Our use of “verifiable” refers to checks over structured fields: schema validity, required-field completeness, object-ID grounding, deterministic rule consistency, trajectory parseability, and expert-derived meta-action agreement. These checks do not certify full natural-language explanation faithfulness or closed-loop driving safety; they expose violations of checkable constraints.

Table 2: Compact verification diagnostics for dataset construction and no-oracle inference. *Dataset diagnostics are computed over final retained VeriDrive train/validation samples after selective correction; no-oracle diagnostics are computed over validation-set autoregressive rollout outputs. Values are reported as percentages over the corresponding samples or rollout chains. Full-chain parse validity measures whether generated  $Q1-Q4$  sequences can be structurally parsed as a complete QA chain, whereas  $\hat{Q}_4$  trajectory parse validity separately checks the final trajectory field satisfies the required numeric trajectory format.*

Diagnostic	Stage	Value
Format validity	Dataset generation	98.7%
Required-field completeness	Dataset generation	97.9%
Attention object-ID validity	Dataset generation	99.1%
$Q_{3E}$ rule consistency	Dataset generation	96.4%
$Q_{3R}$ expert-action agreement	Dataset generation	91.2%
Full-chain parse validity	No-oracle inference	100%
$\hat{Q}_{3P}$ object-ID validity	No-oracle inference	95.5%
$\hat{Q}_{3E}$ checker consistency	No-oracle inference	100%
$\hat{Q}_4$ trajectory parse validity	No-oracle inference	99.0%

Here, required-field completeness checks whether all mandatory structured fields are present,  $Q_{3R}$  expert-action agreement checks whether revision targets match expert-derived meta actions, and no-oracle  $\hat{Q}_{3P}$  object-ID validity checks whether generated object references remain grounded in annotated scene objects. The retained dataset samples are highly checkable across schema, grounding, and rule diagnostics: format validity is 98.7%, required-field completeness is 97.9%, attention object-ID validity is 99.1%, and  $Q_{3E}$  rule consistency is 96.4%. The lower  $Q_{3R}$  expert-action agreement of 91.2% reflects the stricter requirement that revision targets match expert-derived meta actions. During no-oracle rollout, full-chain parse validity and  $\hat{Q}_{3E}$  checker consistency are both 100%, while  $\hat{Q}_4$  trajectory parse validity is 99.0%; the main residual consistency gap is generated object grounding, where  $\hat{Q}_{3P}$  object-ID validity is 95.5%.

## 4.4 Quantitative Results

Table 3 reports the full nuScenes open-loop planning comparison. We keep recent planning and driving-VLM baselines for completeness, but our primary controlled comparison is with OmniDrive [24] under the same Omni-Q setting, because this isolates the effect of the proposed supervision from changes in model architecture or training recipe.

Compared with OmniDrive, filtering (Ours (filter)) reduces average Collision from 0.30 to 0.2411 and average Intersection from 3.00 to 2.0328 (Table 3). At the 3s horizon, Collision decreases from 0.78 to 0.6059 and Intersection from 5.96 to 3.7529. The method also improves 3s  $L_2$  from 0.55 to 0.5343 and average  $L_2$  from 0.33 to 0.3261. Although several recent methods report strong  $L_2$  or Collision values, many do not report Intersection, and they often differ in architecture, training data, or evaluation coverage. We therefore interpret the main evidence as a controlled OmniDrive-to-VeriDrive supervision comparison rather

Table 3: Comparison on nuScenes open-loop planning. *Ego-status indicate BEV/planning-module ego-status injection; - = unreported values. Lower is better. Bottom-block bold values mark the controlled OmniDrive-vs-ours Omni-Q comparison, not global best claims.*

Method	Ego Status		L <sub>2</sub> (m) ↓				Collision (%) ↓				Intersection (%) ↓			
	BEV	Plan	1s	2s	3s	Avg	1s	2s	3s	Avg	1s	2s	3s	Avg
ST-P3 [9] (ECCV 2022)	-	-	1.59	2.64	3.73	2.65	0.69	3.62	8.39	4.23	2.53	8.17	14.40	8.37
UniAD [9] (CVPR 2023)	-	-	0.59	1.01	1.48	1.03	0.16	0.51	1.64	0.77	0.35	1.46	3.99	1.93
UniAD [9] (CVPR 2023)	✓	✓	0.20	0.42	0.75	0.46	0.02	0.25	0.84	0.37	0.20	1.33	3.24	1.59
VAD-Base [9] (ICCV 2023)	-	-	0.69	1.22	1.83	1.25	0.06	0.68	2.52	1.09	1.02	3.44	7.00	3.82
VAD-Base [9] (ICCV 2023)	✓	✓	0.17	0.34	0.60	0.37	0.04	0.27	0.67	0.33	0.21	2.13	5.06	2.47
AD-MLP [9] (CVPR 2024)	-	-	0.15	0.32	0.59	0.35	0.00	0.27	0.85	0.37	0.27	2.52	6.60	2.93
BEV-Planner [9] (CVPR 2024)	-	-	0.30	0.52	0.83	0.55	0.10	0.37	1.30	0.59	0.78	3.79	8.22	4.26
BEV-Planner++ [9] (CVPR 2024)	✓	✓	0.16	0.32	0.57	0.35	0.00	0.29	0.73	0.34	0.35	2.62	6.51	3.16
LAW [9] (ICLR 2025)	-	-	0.26	0.57	1.01	0.61	0.14	0.21	0.54	0.30	-	-	-	-
World4Drive [9] (ICCV 2025)	-	-	0.23	0.47	0.81	0.50	0.02	0.12	0.33	0.16	-	-	-	-
RoboTron-Drive [9] (ICCV 2025)	-	-	0.14	0.30	0.57	0.33	0.03	0.12	0.63	0.26	-	-	-	-
DriveVLM-Dual [9] (CoRL 2025)	-	-	0.15	0.29	0.48	0.31	0.05	0.08	0.17	0.10	-	-	-	-
SOLVE [9] (CVPR 2025)	✓	✓	0.13	0.25	0.47	0.28	0.00	0.16	0.43	0.20	-	-	-	-
OpenDriveVLA-7B [9] (AAAI 2026)	✓	✓	0.20	0.58	1.21	0.66	0.00	0.22	0.55	0.25	-	-	-	-
SparseOccVLA [9] (arXiv 2026)	✓	✓	0.14	0.22	0.32	0.23	0.03	0.12	0.41	0.19	-	-	-	-
OmniDrive [9] (CVPR 2025)	✓	✓	<b>0.14</b>	<b>0.29</b>	0.55	0.33	<b>0.00</b>	0.13	0.78	0.30	0.56	2.48	5.96	3.00
Ours (no filter)	✓	✓	0.1561	0.3091	0.5546	0.3400	0.0000	0.1368	0.6449	0.2606	0.5277	1.8761	3.8695	2.0911
Ours (filter)	✓	✓	0.1489	0.2952	<b>0.5343</b>	<b>0.3261</b>	<b>0.0000</b>	<b>0.1173</b>	<b>0.6059</b>	<b>0.2411</b>	<b>0.5278</b>	<b>1.8178</b>	<b>3.7529</b>	<b>2.0328</b>

than a claim of global superiority across architectures (Table 3).

The comparison among our variants further shows that filtering is complementary to the structured supervision. Relative to our approach with no filter (Ours (no filter)), filtering (Ours (filter)) improves Avg L<sub>2</sub> from 0.3400 to 0.3261, Avg Collision from 0.2606 to 0.2411, and Avg Intersection from 2.0911 to 2.0328 (Table 3).

## 4.5 Qualitative Results

Figure 4 visualizes a representative planning case comparing OmniDrive [24], VeriDrive, and the ground-truth expert ego trajectory. The qualitative comparison complements the open-loop metrics by showing how the proposed supervision changes the generated plan relative to the OmniDrive baseline. In this example, VeriDrive follows the expert trajectory more closely while maintaining consistency with the surrounding scene context. We use this case as an illustrative example of object- and rule-grounded revision supervision, not as an additional quantitative claim.

## 4.6 Ablation Study & Analysis

Tables 4 and 5 summarize the main ablations. Table 4 varies routing budget, key-object count, and counterfactual count, while Table 5 isolates the structured intermediate fields under the no-oracle evaluation protocol.

Group A (Table 4 - left) separates the correction budget from the routing policy. Local-only generation gives the weakest performance, confirming that the local branch alone cannot provide sufficient supervision quality for difficult scenes. Random correction improves over local-only at both 25% and 50%, showing that using more high-quality correction is beneficial even without targeted sample selection. However, validator routing is substantially stronger than random correction at the same budgets: at 25%, it improves L2 from 0.3942 to 0.3294, Collision from 0.3396 to 0.2468, and Intersection from 2.1398 to 2.0417; at 50%, it improves L2 from 0.3647 to 0.3265, Collision from 0.3062 to 0.2414, and Intersection from 2.1065 to 2.0344 (Table 4 - left). This indicates that the validator does not merely increase correction budget, but allocates it to samples with higher expected supervision gain. 100% All-GPT provides an expensive upper-bound reference achieving the best Collision, while



Figure 4: Qualitative planning comparison. In each row, the left panels show the multi-view scene context and the right panel shows the BEV trajectory visualization. Gray dots (●) denote the ground-truth expert trajectory (GT), red square/dot markers (■/●) denote the OmniDrive prediction, and green diamond/dot markers (◆/●) denote the VeriDrive prediction. The black star (★) marks the ego origin; blue boxes (□) and gray boxes (□) denote moving and static object boxes, respectively; cyan dashed curves show moving-object future trajectories. Upper: VeriDrive produces a trajectory closer to the expert path than OmniDrive in the night intersection case. Lower: VeriDrive better follows the expert left-turn trajectory in the daytime intersection case under the same scene context.

the default 30%<sup>†</sup> validator-routed setting achieving better L2 and Intersection with much lower correction usage (Table 4 - left).

Table 4: Component ablations on average nuScenes open-loop metrics. Group A compares correction budgets and same-budget random controls; Ratio is the escalation proportion. The superscript <sup>†</sup> marks the default VeriDrive setting, i.e., 30% validator routing used in the main experiments. Group B varies the number of selected key objects  $K$ , and Group C varies the number of counterfactual trajectories  $T$ . Lower is better; Coll./Inter. denote average Collision/Intersection.

A: routing and correction budget					B/C: key objects and counterfactual count				
Ratio	Policy	L2 ↓	Coll. ↓	Inter. ↓	Group	Setting	L2 ↓	Coll. ↓	Inter. ↓
0%	Local only	0.4478	0.3749	2.1764	B	$K = 3$	0.5896	0.4138	2.4517
25%	Random correction	0.3942	0.3396	2.1398	B	$K = 5$	<b>0.3261</b>	<b>0.2411</b>	<b>2.0328</b>
25%	Validator routing	0.3294	0.2468	2.0417	B	$K = 8$	0.3389	0.2597	2.0794
50%	Random correction	0.3647	0.3062	2.1065	C	$T = 1$	<b>0.3261</b>	<b>0.2411</b>	<b>2.0328</b>
50%	Validator routing	0.3265	0.2414	2.0344	C	$T = 2$	0.3354	0.2575	2.0593
100%	All-GPT correction	0.3268	0.2161	2.0573	C	$T = 4$	0.3336	0.2558	2.0478
30% <sup>†</sup>	<i>Ours (filter)</i>	<b>0.3261</b>	<b>0.2411</b>	<b>2.0328</b>					

Groups B and C (Table 4 - right) show that compact evidence is preferable in this setting. Keeping  $K = 5$  key objects outperforms both  $K = 3$  and  $K = 8$ , and one counterfactual trajectory is sufficient; adding more simulated trajectories does not improve the reported open-loop metrics.

Table 5: Ablation on structured intermediate supervision under no-oracle autoregressive evaluation. Numbers are Avg L2 / Avg Collision / Avg Intersection.  $Q_{3E}$  is not evaluated alone because it depends on  $Q_{3P}$  object-centric future motion grounding.

Setting	$Q_{3P}$	$Q_{3E}$	$Q_{3R}$	Avg L2 ↓ / Avg Coll. ↓ / Avg Inter. ↓
Q4 only / w/o structured CoT	–	–	–	0.3912 / 0.3602 / 2.3569
+ object future motion grounding	✓	–	–	0.3834 / 0.3187 / 2.2974
+ rule-grounded evaluation	✓	✓	–	0.3470 / 0.3048 / 2.0980
Full VeriDrive	✓	✓	✓	0.3261 / 0.2411 / 2.0328

Table 5 shows that future grounding, rule-grounded evaluation, and expert-aligned revision provide complementary supervision.  $Q_{3P}$  supplies object-level future interaction evidence,  $Q_{3E}$  converts this evidence into rule-grounded risk diagnosis,  $Q_{3R}$  teaches how risky/invalid intent should be revised toward the expert behavior. The full model performs the best overall L2, Collision, and Intersection values, indicating that diagnosis alone is insufficient unless paired with revision supervision that bridges failure attribution and final planning.

Table 6 reports project-level generation overhead and estimated paid GPT API cost. Compared with the reproduced OmniDrive-style [24] single-GPT construction baseline under the same accounting, our filtered approach (Ours (filter) - Table 6) reduces the total project token budget from 256.6M to 157.3M tokens and the total generation time from 290.0 hours to 208.2 hours. The estimated paid GPT API cost is reduced from \$2.69k to \$0.54k because the proposed pipeline uses local generation for most samples and routes only about 30% of samples to the GPT correction branch. Ours (no filter) already reduces token and time overhead through compact scene conditioning, while Ours (filter) further improves the efficiency–performance trade-off by combining structured validation with selective correction. The cost column counts only paid GPT API calls; local Qwen3-VL inference is reflected in logged time rather than converted to a hardware-normalized dollar cost.

Table 6: Project-level generation efficiency and estimated paid GPT API cost comparison. Token and time columns report total logged pipeline overhead, including local generation and any invoked correction. Est. GPT cost is computed from logged GPT input/output tokens using GPT-5.5 standard API pricing of \$5.00/1M input tokens and \$30.00/1M output tokens, without cached-input, Batch, Flex, or Priority discounts. The OmniDrive-style row denotes our cost-normalized single-GPT baseline under the same pricing basis, rather than the original OmniDrive authors’ reported data-generation cost. For Ours, the estimate applies the 30% high-quality routing ratio. Local Qwen3-VL inference is included in logged generation time but is not converted to a hardware-normalized dollar cost.

Pipeline	Samples	GPT ratio	Total tok. /sample	Time /sample	Project tok. (M)	Project time (h)	Est. GPT cost (USD)
OmniDrive-style single-GPT	34.1k	100%	7524.3	30.62s	256.6	290.0	\$2.69k
Ours (no filter)	33.1k	30%	5421.1	25.85s	179.6	238.0	\$0.57k
Ours (filter)	33.1k	30%	4746.2	22.62s	157.3	208.2	\$0.54k

## 5 Conclusion

We presented VeriDrive, a framework for constructing programmatically verifiable counterfactual supervision for vision-language planning. By decomposing driving reasoning into compact scene evidence, ego meta action, object-centric future grounding, rule-grounded counterfactual evaluation, expert-aligned revision, and final planning, VeriDrive turns free-form driving rationales into auditable intermediate supervision. The framework also introduces a low-cost generation pipeline that combines compact scene conditioning, local generation, dual validation, and selective GPT correction. Using this pipeline, we construct the VeriDrive dataset on top of nuScenes, providing structured QA supervision and edit traces for object- and rule-grounded planning. Experiments show that this supervision improves L2, Collision, and Intersection relative to the state-of-the-art counterfactual-supervision baseline OmniDrive [24] while reducing logged token usage, generation time, and estimated paid GPT API cost. Overall, VeriDrive suggests that structured verifiability and budget-aware generation can make driving-VLM supervision more auditable, scalable, and reproducible.

**Future work:** VeriDrive structured supervision opens several natural extensions. First, its validators can be expanded with richer traffic-rule libraries and temporal-consistency checks, enabling more fine-grained auditing of multi-agent interactions. Second, the budget-aware routing policy can be made adaptive to model uncertainty and scene difficulty, allocating high-quality generation where it is most informative. Third, the same Perception–Evaluation–Revision interface can be transferred to broader driving backbones, additional driving datasets, and interactive simulation platforms, turning verifiable supervision into a reusable auditing layer for vision-language planning.

## References

- [1] Shuai Bai et al. Qwen3-VL technical report. *arXiv preprint arXiv:2511.21631*, 2025.
- [2] Holger Caesar, Varun Bankiti, Alex H. Lang, Sourabh Vora, Venice Erin Liong, Qiang Xu, Anush Krishnan, Yu Pan, Giancarlo Baldan, and Oscar Beijbom. nuScenes: A multimodal dataset for autonomous driving. In *Proceedings of the IEEE/CVF Conference on Computer Vision and Pattern Recognition (CVPR)*, pages 11621–11631, 2020.

- [3] Xuesong Chen, Linjiang Huang, Tao Ma, Rongyao Fang, Shaoshuai Shi, and Hongsheng Li. SOLVE: Synergy of language-vision and end-to-end networks for autonomous driving. In *Proceedings of the IEEE/CVF Conference on Computer Vision and Pattern Recognition (CVPR)*, pages 12068–12077, 2025.
- [4] Chenxu Dang, Jie Wang, Guang Li, Zhiwen Hou, Zihan You, Hangjun Ye, Jie Ma, Long Chen, and Yan Wang. Sparseocclva: Bridging occupancy and vision-language models via sparse queries for unified 4d scene understanding and planning. *arXiv preprint arXiv:2601.06474*, 2026.
- [5] Thierry Deruyttere, Simon Vandenhende, Dusan Grujicic, Luc Van Gool, and Marie-Francine Moens. Talk2car: Taking control of your self-driving car. In *Proceedings of the 2019 Conference on Empirical Methods in Natural Language Processing and the 9th International Joint Conference on Natural Language Processing (EMNLP-IJCNLP)*, pages 2088–2098, 2019. doi: 10.18653/v1/D19-1215.
- [6] Yuxin Fang, Quan Sun, Xinggong Wang, Tiejun Huang, Xinlong Wang, and Yue Cao. EVA-02: A visual representation for neon genesis. *Image and Vision Computing*, 149: 105171, 2024. doi: 10.1016/j.imavis.2024.105171.
- [7] Shengchao Hu, Li Chen, Penghao Wu, Hongyang Li, Junchi Yan, and Dacheng Tao. ST-P3: End-to-end vision-based autonomous driving via spatial-temporal feature learning. In *Computer Vision – ECCV 2022*, pages 533–549, 2022. doi: 10.1007/978-3-031-19839-7\_31.
- [8] Yihan Hu, Jiazhi Yang, Li Chen, Keyu Li, Chonghao Sima, Xizhou Zhu, Siqi Chai, Senyao Du, Tianwei Lin, Wenhai Wang, Lewei Lu, Xiaosong Jia, Qiang Liu, Jifeng Dai, Yu Qiao, and Hongyang Li. UniAD: Planning-oriented autonomous driving. In *Proceedings of the IEEE/CVF Conference on Computer Vision and Pattern Recognition (CVPR)*, pages 17853–17862, 2023.
- [9] Zhijian Huang, Chengjian Feng, Feng Yan, Baihui Xiao, Zequn Jie, Yujie Zhong, Xiaodan Liang, and Lin Ma. Robotron-drive: All-in-one large multimodal model for autonomous driving. In *Proceedings of the IEEE/CVF International Conference on Computer Vision (ICCV)*, pages 8011–8021, 2025.
- [10] Bo Jiang, Shaoyu Chen, Qing Xu, Bencheng Liao, Jiajie Chen, Helong Zhou, Qian Zhang, Wenyu Liu, Chang Huang, and Xinggong Wang. VAD: Vectorized scene representation for efficient autonomous driving. In *Proceedings of the IEEE/CVF International Conference on Computer Vision (ICCV)*, pages 8340–8350, 2023.
- [11] Jinkyu Kim, Anna Rohrbach, Trevor Darrell, John Canny, and Zeynep Akata. Textual explanations for self-driving vehicles. In *Proceedings of the European Conference on Computer Vision (ECCV)*, pages 563–578, 2018.
- [12] Yingyan Li, Lue Fan, Jiawei He, Yuqi Wang, Yuntao Chen, Zhaoxiang Zhang, and Tieniu Tan. Enhancing end-to-end autonomous driving with latent world model. In *International Conference on Learning Representations (ICLR)*, 2025.
- [13] Zhiqi Li, Zhiding Yu, Shiyi Lan, Jiahao Li, Jan Kautz, Tong Lu, and Jose M. Alvarez. Is ego status all you need for open-loop end-to-end autonomous driving? In *Proceedings*

- of the *IEEE/CVF Conference on Computer Vision and Pattern Recognition (CVPR)*, pages 14864–14873, 2024.
- [14] Haotian Liu, Chunyuan Li, Yuheng Li, and Yong Jae Lee. Improved baselines with visual instruction tuning. In *Proceedings of the IEEE/CVF Conference on Computer Vision and Pattern Recognition (CVPR)*, pages 26296–26306, 2024.
- [15] Srikanth Malla, Chiho Choi, Isht Dwivedi, Joon Hee Choi, and Jiachen Li. DRAMA: Joint risk localization and captioning in driving. In *Proceedings of the IEEE/CVF Winter Conference on Applications of Computer Vision (WACV)*, pages 1043–1052, 2023.
- [16] Ana-Maria Marcu, Long Chen, Jan Hünemann, Alice Karnsund, Benoit Hanotte, Prajwal Chidananda, Saurabh Nair, Vijay Badrinarayanan, Alex Kendall, Jamie Shotton, Elahe Arani, and Oleg Sinavski. Lingoqa: Visual question answering for autonomous driving. In *Computer Vision – ECCV 2024*, pages 252–269, 2024. doi: 10.1007/978-3-031-72980-5\_15.
- [17] Ming Nie, Renyuan Peng, Chunwei Wang, Xinyue Cai, Jianhua Han, Hang Xu, and Li Zhang. Reason2drive: Towards interpretable and chain-based reasoning for autonomous driving. In *Computer Vision – ECCV 2024*, pages 292–308, 2024. doi: 10.1007/978-3-031-73347-5\_17.
- [18] Tianwen Qian, Jingjing Chen, Linhai Zhuo, Yang Jiao, and Yu-Gang Jiang. Nuscenesqa: A multi-modal visual question answering benchmark for autonomous driving scenario. In *Proceedings of the AAAI Conference on Artificial Intelligence (AAAI)*, volume 38, pages 4542–4550, 2024. doi: 10.1609/aaai.v38i5.28253.
- [19] Vasili Ramanishka, Yi-Ting Chen, Teruhisa Misu, and Kate Saenko. Toward driving scene understanding: A dataset for learning driver behavior and causal reasoning. In *Proceedings of the IEEE/CVF Conference on Computer Vision and Pattern Recognition (CVPR)*, pages 7699–7707, 2018.
- [20] Enna Sachdeva, Nakul Agarwal, Suhas Chundi, Sean Roelofs, Jiachen Li, Mykel Kochenderfer, Chiho Choi, and Behzad Dariush. Rank2tell: A multimodal driving dataset for joint importance ranking and reasoning. In *Proceedings of the IEEE/CVF Winter Conference on Applications of Computer Vision (WACV)*, pages 7513–7522, 2024.
- [21] Chonghao Sima, Katrin Renz, Kashyap Chitta, Li Chen, Hanxue Zhang, Chengen Xie, Jens Beißwenger, Ping Luo, Andreas Geiger, and Hongyang Li. DriveLM: Driving with graph visual question answering. In *Computer Vision – ECCV 2024*, pages 256–274, 2024.
- [22] Xiaoyu Tian, Junru Gu, Bailin Li, Yicheng Liu, Yang Wang, Zhiyong Zhao, Kun Zhan, Peng Jia, XianPeng Lang, and Hang Zhao. Drivevlm: The convergence of autonomous driving and large vision-language models. In *Proceedings of The 8th Conference on Robot Learning*, pages 4698–4726, 2025.
- [23] Huijie Wang, Tianyu Li, Yang Li, Li Chen, Chonghao Sima, Zhenbo Liu, Bangjun Wang, Peijin Jia, Yuting Wang, Shengyin Jiang, Feng Wen, Hang Xu, Ping Luo, Junchi

- Yan, Wei Zhang, and Hongyang Li. OpenLane-V2: A topology reasoning benchmark for unified 3d hd mapping. In *Advances in Neural Information Processing Systems (NeurIPS)*, volume 36, 2023.
- [24] Shihao Wang, Zhiding Yu, Xiaohui Jiang, Shiyi Lan, Min Shi, Nadine Chang, Jan Kautz, Ying Li, and Jose M. Alvarez. OmniDrive: A holistic vision-language dataset for autonomous driving with counterfactual reasoning. In *Proceedings of the IEEE/CVF Conference on Computer Vision and Pattern Recognition (CVPR)*, pages 22442–22452, June 2025.
- [25] Dongming Wu, Wencheng Han, Yingfei Liu, Tiancai Wang, Cheng-Zhong Xu, Xiangyu Zhang, and Jianbing Shen. Language prompt for autonomous driving. In *Proceedings of the AAAI Conference on Artificial Intelligence*, volume 39, pages 8359–8367, 2025. doi: 10.1609/aaai.v39i8.32902.
- [26] Yiran Xu, Xiaoyin Yang, Lihang Gong, Hsuan-Chu Lin, Tz-Ying Wu, Yunsheng Li, and Nuno Vasconcelos. Explainable object-induced action decision for autonomous vehicles. In *Proceedings of the IEEE/CVF Conference on Computer Vision and Pattern Recognition (CVPR)*, pages 9523–9532, 2020. doi: 10.1109/CVPR42600.2020.00954.
- [27] Yuqi Ye, Zijian Zhang, Junhong Lin, Shangkun Sun, Changhao Peng, and Wei Gao. AutoDrive-P<sup>3</sup>: Unified chain of perception–prediction–planning thought via reinforcement fine-tuning. In *International Conference on Learning Representations (ICLR)*, 2026. Poster.
- [28] Jiang-Tian Zhai, Ze Feng, Jinhao Du, Yongqiang Mao, Jiang-Jiang Liu, Zichang Tan, Yifu Zhang, Xiaoqing Ye, and Jingdong Wang. Rethinking the open-loop evaluation of end-to-end autonomous driving in nuScenes. *arXiv preprint arXiv:2305.10430*, 2023. doi: 10.48550/arXiv.2305.10430.
- [29] Yupeng Zheng, Pengxuan Yang, Zebin Xing, Qichao Zhang, Yuhang Zheng, Yinfeng Gao, Pengfei Li, Teng Zhang, Zhongpu Xia, Peng Jia, XianPeng Lang, and Dongbin Zhao. World4drive: End-to-end autonomous driving via intention-aware physical latent world model. In *Proceedings of the IEEE/CVF International Conference on Computer Vision (ICCV)*, pages 28632–28642, 2025.
- [30] Xingcheng Zhou, Xuyuan Han, Feng Yang, Yunpu Ma, Volker Tresp, and Alois Knoll. Opendrivevla: Towards end-to-end autonomous driving with large vision language action model. In *Proceedings of the AAAI Conference on Artificial Intelligence (AAAI)*, volume 40, pages 13782–13790, 2026. doi: 10.1609/aaai.v40i16.38386.

## A Supplementary Material

This supplement provides efficiency details and implementation details that complement the main paper. The main paper emphasizes the methodological contribution of VeriDrive and keeps the engineering description intentionally compact. This supplement consolidates the reproducibility-oriented details that are useful for implementation, including: (1) how the structured supervision tuple is serialized during training and inference, (2) which models and thresholds are used in the data generation pipeline, and (3) the optimization settings used in the final fine-tuning stage.

## B Training and Inference Serialization

For each scene, VeriDrive constructs a structured supervision tuple

$$\mathcal{Q} = \{Q_1, Q_2, Q_{3P}, Q_{3E}, Q_{3R}, Q_4\},$$

where  $Q_1$  is the compact planning-oriented scene evidence,  $Q_2$  is the ego meta action,  $Q_{3P}$  is the object-centric future motion grounding,  $Q_{3E}$  is the rule-grounded counterfactual evaluation,  $Q_{3R}$  is the expert-aligned revision target, and  $Q_4$  is the final expert planning target.

During Stage-3 training, we use the verified intermediate fields as teacher-forced supervision in the structured sequence

$$Q_1 \rightarrow Q_2 \rightarrow Q_{3P} \rightarrow Q_{3E} \rightarrow Q_{3R} \rightarrow Q_4.$$

These fields expose the model to object-grounded future motion evidence, rule-grounded counterfactual evaluation, and expert-aligned revision supervision without changing the information available during evaluation. Equivalently, the training sequence can be summarized as

$$\underbrace{[Q_1; Q_2; Q_{3P}; Q_{3E}; Q_{3R}]}_{\text{teacher-forced structured supervision}} \rightarrow \underbrace{[Q_4]}_{\text{final planning target}}. \quad (8)$$

At inference time, VeriDrive follows the no-oracle autoregressive rollout used in the main paper. The model is given only the normal scene observation inputs used by the Omni-Q setting, together with current ego/map context when available in the baseline protocol, and sequentially generates

$$\hat{Q}_1 \rightarrow \hat{Q}_2 \rightarrow \hat{Q}_{3P} \rightarrow \hat{Q}_{3E} \rightarrow \hat{Q}_{3R} \rightarrow \hat{Q}_4.$$

Ground-truth future object trajectories, rule-evaluation labels, expert meta-actions, and revision targets are not supplied during evaluation. Thus,  $Q_{3P}$ ,  $Q_{3E}$ , and  $Q_{3R}$  are training-time supervision fields rather than oracle test-time inputs.

## C Compact Scene Conditioning

The compact context used in VeriDrive is designed to reduce prompt redundancy while retaining planning-critical evidence. We apply rule-based filtering before serialization and use the following defaults throughout the experiments:

- $\text{key\_objects} \leq 5$ , selected according to lane relation, spatial proximity, vulnerable-road-user status, and traffic-control relevance.
- $\text{key\_traffic} \leq 2$ , with traffic signals and crosswalks prioritized when they are present and relevant to the ego plan.
- Ego future supervision represented by 6 trajectory steps.
- Each selected surrounding object represented by a 12-step future trajectory for interaction grounding.

The compact evidence space is

$$\mathcal{C}_n = \left\{ \mathcal{C}_n^{\text{road}}, \mathcal{C}_n^{\text{traffic}}, \mathcal{O}_n^{\text{key}} \right\}.$$

Candidate objects are scored with

$$\Theta = \left\{ \theta^{\text{lane}}, \theta^{\text{prox}}, \theta^{\text{vru}}, \theta^{\text{ctrl}} \right\}, \quad r_i = \sum_{\theta \in \Theta} w_\theta \theta(o_i),$$

where the attributes measure lane relevance, interaction proximity, vulnerable-road-user priority, and traffic-control coupling. We use uniform weights unless otherwise stated and retain

$$\mathcal{O}_n^{\text{key}} = \text{TopK} \left( \{r_i\}_{i=1}^{N_n}, K_{\text{max}} \right).$$

After filtering out samples without valid expert trajectories, the VeriDrive dataset contains 27,271 training samples and 5,868 validation samples. The resulting QA tuples are fully scriptable from nuScenes and OpenLane-V2 annotations, which makes the data construction pipeline easier to reproduce than free-form annotation schemes.

## D Data Generation Pipeline Details

The budget-aware generation pipeline uses three model roles:

- **Local generator:** Qwen3-VL-32B-Instruct.
- **High-quality generator:** GPT-5.5.
- **Auxiliary judge:** GPT-5 mini.

The local branch handles the majority of samples and is paired with a dual-branch validator. The validator checks both structural correctness and agreement with deterministic references. The thresholds used in the main experiments are:

- trajectory consistency threshold  $\text{tol\_traj} = 0.5$ ;
- reference agreement threshold  $\text{tol\_ref} = 1.0$ ;
- complexity threshold  $\tau_p = 0.65$  when selective routing is enabled.

Operationally, invalid samples are always escalated to the expensive branch for repair. Valid but difficult samples are escalated only when their estimated complexity exceeds  $\tau_p$  and the available budget permits correction. This keeps the expensive branch focused on the subset of samples where higher-quality generation is most likely to improve the final supervision.

## E Implementation Settings

Table 7: Reproducibility-oriented implementation settings used in VeriDrive.

Component	Setting	Component	Setting
Architecture	Omni-Q following OmniDrive	Epochs	2
Visual encoder	EVA-02-L	GPUs	2
Language backbone	LLaVA v1.5-based	<code>samples_per_gpu</code>	4
Stage-3 optimizer	AdamW	Global batch size	8
Learning rate	$2 \times 10^{-5}$	Local generator	Qwen3-VL-32B-Instruct
Weight decay	$10^{-4}$	High-quality generator	GPT-5.5
<code>tol_traj</code>	0.5	Judge model	GPT-5 mini
<code>tol_ref</code>	1.0	<code>key_objects</code>	$\leq 5$
Complexity threshold	0.65	<code>key_traffic</code>	$\leq 2$

## F Optimization Details

We adopt the Omni-Q architecture of OmniDrive [24], with EVA-02-L as the visual encoder and a LLaVA v1.5-based language backbone. To isolate the effect of the proposed supervision, we keep the original Stage-1 (2D pretraining) and Stage-2 (3D fine-tuning) settings unchanged, and only modify the Stage-3 training data.

Stage-3 fine-tuning is performed for 2 epochs using AdamW with learning rate  $2 \times 10^{-5}$  and weight decay  $10^{-4}$ . Training runs on 2 GPUs with `samples_per_gpu`=4, which gives a global batch size of 8. We initialize from the OmniDrive pretrained checkpoint and use the structured serialization protocol described above without changing the backbone architecture or the optimizer family.

## G Practical Reproduction Notes

For a faithful reproduction of the reported results, the following implementation choices matter most:

- Use the same OmniDrive initialization and Stage-1/Stage-2 recipe before introducing VeriDrive supervision in Stage-3.
- Keep compact scene filtering enabled so that the structured evidence space matches the data-generation prompts and the training serialization.
- Do not externally provide ground-truth  $Q_2$ ,  $Q_{3P}$ ,  $Q_{3E}$ , or  $Q_{3R}$  at evaluation time; they should be generated by the model before the final plan  $Q_4$ .
- Keep the validator thresholds fixed when comparing routing strategies, otherwise quality and cost comparisons become less meaningful.

## H Detailed Token Breakdown

The main paper reports project-level token usage, generation time, and estimated paid GPT API cost in Table 6; here we provide the desc/VQA component breakdown.

Setting	Input	Output	Total	Time(s/sample)
<b>Reproduced OmniDrive-style pipeline (GPT-5.5 single generation)</b>				
desc	2573.8	289.5	2863.3	8.20
vqa	3302.6	1358.4	4661.0	22.42
total	5876.4	1647.9	7524.3	30.62
<b>Ours (Qwen3-VL-32B-Instruct + GPT-5.5 hybrid generation)</b>				
<b>desc</b>	<b>1870.6</b>	<b>229.6</b>	<b>2100.2</b>	<b>5.89</b>
vqa (no filter)	2326.7	994.2	3320.9	19.96
total (no filter)	4197.3	1223.8	5421.1	25.85
<b>vqa (+filter)</b>	<b>1664.0</b>	<b>982.0</b>	<b>2646.0</b>	<b>16.73</b>
total (+filter)	3534.6	1211.6	4746.2	22.62

Table 8: Detailed token-consumption breakdown per sample between a reproduced OmniDrive-style single-GPT baseline and our hybrid pipeline. The OmniDrive-style baseline is cost-normalized under the same GPT-5.5 pricing basis and does not denote the original OmniDrive authors’ reported generation cost. Our hybrid pipeline uses Qwen3-VL-32B-Instruct and GPT-5.5 with a routing assumption of 70% Qwen and 30% GPT.

## I Additional Qualitative Visualizations



Figure 5: Additional qualitative visualization from VeriDrive.



Figure 6: Additional qualitative visualization from VeriDrive.



Figure 7: Additional qualitative visualization from VeriDrive.